
Causality for Tabular Data Synthesis: A High-Order Structure Causal Benchmark Framework

Ruibo Tu[‡], Zineb Senane[‡], Lele Cao^{*}, Cheng Zhang[†], Hedvig Kjellström[‡], Gustav Eje Henter[‡]

Abstract

Tabular synthesis models remain ineffective at capturing complex dependencies, and the quality of synthetic data is still insufficient for comprehensive downstream tasks, such as prediction under distribution shifts, automated decision-making, and cross-table understanding. A major challenge is the lack of prior knowledge about underlying structures and high-order relationships in tabular data. We argue that a systematic evaluation on high-order structural information for tabular data synthesis is the first step towards solving the problem. In this paper, we introduce high-order structural causal information as natural prior knowledge and provide a benchmark framework for the evaluation of tabular synthesis models. The framework allows us to generate benchmark datasets with a flexible range of data generation processes and to train tabular synthesis models using these datasets for further evaluation. We propose multiple benchmark tasks, high-order metrics, and causal inference tasks as downstream tasks for evaluating the quality of synthetic data generated by the trained models. Our experiments demonstrate to leverage the benchmark framework for evaluating the model capability of capturing high-order structural causal information. Furthermore, our benchmarking results provide an initial assessment of state-of-the-art tabular synthesis models. They have clearly revealed significant gaps between ideal and actual performance and how baseline methods differ. Our benchmark framework is available at URL <https://github.com/TURuibo/CauTabBench>.

1 Introduction

Tabular data are common and essential in both industries and natural sciences; whereas, tabular domain in machine learning has been overlooked [van Breugel and van der Schaar, 2024]. Among tasks in tabular domain, tabular data synthesis is an important one with many applications, such as augmentation to address data scarcity issues [Choi et al., 2017], pretraining for downstream tasks [Hollmann et al., 2023], and privacy protection [Hernandez et al., 2022]. Recently, the quality of synthetic tabular data has significantly improved with deep diffusion models (DFMs) [Ho et al., 2020] and large language models (LLMs) [Brown et al., 2020].

Nevertheless, tabular data synthesis still faces many challenges. These challenges can be organized into three classes: (i) handling practical issues, such as mixed data types [Ma et al., 2020] and missing data; (ii) capturing structural information intrinsic to the nature of tabular data, especially high-order instance and feature dependencies [Li et al., 2023]; (iii) synthesis in a cross-table setting, such as capturing the dependencies across different tables [Scetbon et al., 2024]. Many works handle practical issues [Kotelnikov et al., 2023, Kim et al., 2023, Lee et al., 2023, Zhang et al., 2024], which need to be solved first for training synthesis models. In contrast, few works focus on high-order information that is more important for complicated real-world applications, such as in-context prediction [Zhu et al., 2023b, Hollmann et al., 2023], and generalization and analysis of multiple tables [Wang and Sun, 2022, Zhu et al., 2023a].

^{*}King (part of Microsoft), Stockholm, Sweden. [†]: Microsoft Research, Cambridge, UK. [‡]: KTH Royal Institute of Technology, Stockholm, Sweden; emails: ruibo@kth.se.

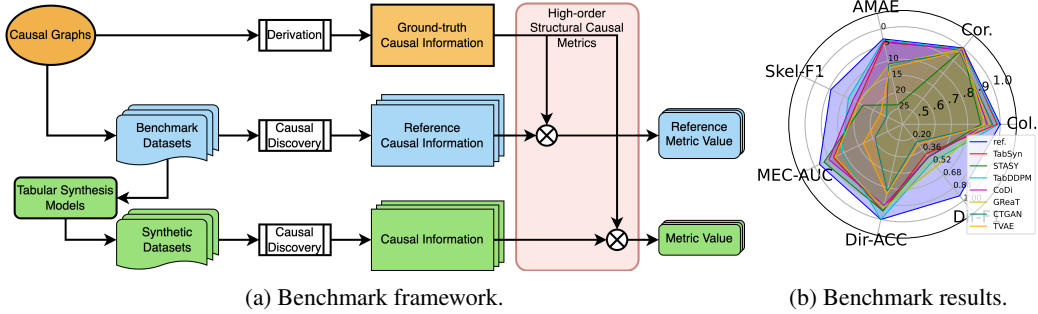


Figure 1: Our high-order structural causal benchmark framework and results. Benchmark datasets are generated based on randomly sampled causal graphs that also are used for deriving ground-truth causal information. Benchmark datasets are used for training tabular synthesis models, which generate synthetic datasets. To evaluate synthesis models on high-order structural causal information, we extract causal information from benchmark and synthetic datasets using causal discovery methods and then apply high-order structural causal metrics to compare to the known ground-truth causal information. Benchmark results demonstrate the performance of baseline methods with different metrics. The metric values computed on benchmark datasets are used as references.

One reason for the lack of studies could be the absence of a systematic evaluation of synthesis models on high-order information. This absence not only creates a limited and misleading impression of the performance of synthesis models, but also hinders the development and application of high-order information-aware synthesis models. The evaluation of tabular synthesis models is an active research area [van Breugel and van der Schaar, 2023]. Currently, it is mainly based on the performance of using synthetic data for downstream tasks [van Breugel and van der Schaar, 2024], known as *extrinsic evaluation* [Bommasani et al., 2021]. Extrinsic evaluation only provides a limited understanding of tabular synthesis models restricted by the downstream tasks. In contrast, *intrinsic evaluation* directly evaluates the quality of synthetic data, such as the metrics defined with lower-order statistics (pair-wise correlation-based scores). Helpful intrinsic evaluation, especially metrics with high-order information, is difficult in the tabular domain, since it always relies on informative prior knowledge that is lack of studies in the tabular domain [van Breugel and van der Schaar, 2024].

To benchmark models on high-order structural information, we propose to leverage the study of causal graphical models [Spirtes et al., 2000, Peters et al., 2017] that have applied causal prior knowledge for a wide range of machine learning applications [Pearl et al., 2016, Schölkopf et al., 2021] and are still under-explored in tabular domain. We consider causal graphs as a natural and compact representation of high-order structural information about causal dependencies in tabular data. A few works [Choi et al., 2020, Liu et al., 2023, Yan et al., 2023] have attempted to use general graph properties (e.g., adjacency matrices and directed acyclicity) for representation learning and tabular data synthesis, but all neglect to consider high-order structural causal information. In contrast, this work aims to create the foundation that covers the essential and necessary aspects for benchmarking tabular synthesis models on high-order structural causal information and demonstrate how to utilize benchmarking results to guide future improvements in tabular synthesis models. More specifically, we

1. introduce high-order structural causal information as prior knowledge for modelling dependencies among the variables of interest in tabular data. We characterize the information into three levels for benchmarking tabular synthesis models (Sec. 3);
2. propose a benchmark framework for the evaluation of tabular synthesis models on high-order structural causal information, which is summarized in Fig. 1. Specifically, we illustrate how to generate benchmark datasets and how high-order structural causal tasks and downstream causal-inference tasks can be used for evaluation (Sec. 4);
3. demonstrate to utilize our framework for evaluating state-of-the-art DFM- and LLM-based tabular synthesis models on benchmark datasets and on real-world datasets (Sec. 5 and App. D). Our experimental results in a limited setting have already shown the gap between the ideal and actual performance of baseline methods distinctly and highlighted their shortcomings

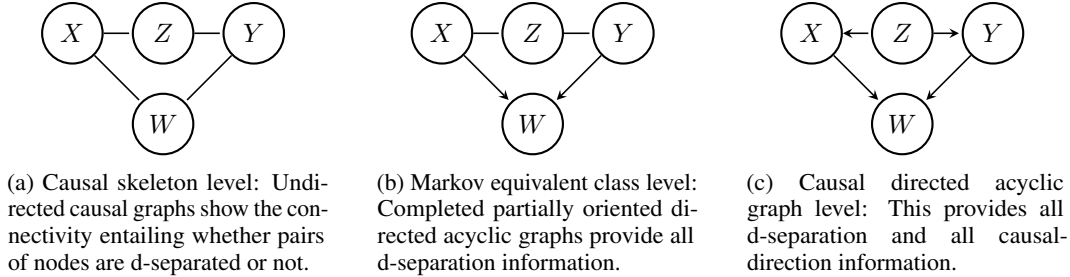


Figure 2: Three levels of high-order structural causal information.

from various perspectives. We discuss limitations and future works involving expanding the framework for more comprehensive and large-scale evaluations in App. B.

2 Related Work

To understand tabular data models from different perspectives, and to make progress towards better real-world performance, a suite of benchmarks with different purposes is needed. In prior benchmarking efforts, Grinsztajn et al. [2022] use diverse tabular datasets for investigating the performance of tree-based methods; Bommert et al. [2020], Passemiers et al. [2023], Cherepanova et al. [2023] contribute benchmark datasets to the studies of feature selection; Malinin et al. [2021], Gardner et al. [2023] focus on the robustness to distribution shifts. Moreover, to bridge the gap between real-world applications and synthetic data, Jesus et al. [2022] provide a larger scale tabular dataset in finance including practical challenges. In contrast, Qian et al. [2023] provide a number of synthetic data generators for a better model development by avoiding practical issues of real-world data, such as selection bias and missing value issues. Furthermore, in the context of tabular data synthesis, Hansen et al. [2023] introduce data-centric AI techniques which can provide data profiles, and then propose an evaluation framework to show the importance of integrating data profiles into synthesis models. Different from previous efforts, our work provides a new perspective for understanding and improving tabular synthesis models by benchmarking on high-order structural causal information.

Tabular data synthesis was initially based on classical deep generative models [Jordon et al., 2018, Xu et al., 2019, Morales-Alvarez et al., 2022], but has recently flourished with Transformer-based, LLM-based, and DFM-based methods. For example, to generate synthetic tabular data, [Gulati and Roysdon, 2023] applies a masked Transformer [Vaswani et al., 2017]; *GReaT* [Borisov et al., 2022] formulates tabular data as sentences and finetunes Generative Pre-trained Transformer 2 (GPT-2) [Radford et al., 2019]; *TabDDPM* [Kotelnikov et al., 2023], and *CoDi* [Lee et al., 2023] apply denoising diffusion probabilistic models [Ho et al., 2020]; *STaSy* [Kim et al., 2023] uses a score-based diffusion model [Song and Ermon, 2019]; *Forest-VP* and *Forest-Flow* [Jolicoeur-Martineau et al., 2024] use tree-based [Chen et al., 2015] deep diffusion and flow matching models [Lipman et al., 2023]. Additionally, *GOGGLE* [Liu et al., 2023] uses an encoder-decoder model for generating tabular data, of which the decoder is a graph neural network to capture the dependencies between features. Since more and more tabular synthesis models are introduced every day, we mainly mentioned the representative ones for each category and benchmark on most of them in the experiments. Nevertheless, we highly suggest survey papers [Borisov et al., 2022, Li et al., 2023, Fang et al., 2024] for more detail about tabular synthesis models.

3 High-Order Structural Causal Information

A fundamental problem in modeling tabular data is the lack of prior knowledge about their structures and high-order information [Borisov et al., 2022, Fang et al., 2024]. Natural and common prior knowledge in tabular domain can be causal dependencies in forms of causal graphs [Peters et al., 2017, Glymour and Zhang, 2019]. Because real-world data are generated according to some mechanisms and causal graphs are used for qualitatively describing data generation processes. As for tabular data whose columns are variables of interests, *causal graphs* are directed graphs where the nodes are variables and the directed edges represent causal relationships between the columns. Different

from mere pair-wise information (e.g., correlations), such causal relationships represent high-order structural information. And to capture it requires more than pair-wise reasoning and pair-wise methods. We assume that the causal graphs are directed acyclic graphs (DAGs) and that there are no unknown confounders. These are common assumptions in causal machine learning [Peters et al., 2017, Schölkopf et al., 2021] under which the studies are significantly supported by well-studied properties and theories as well as reliable methods and considerable applications. Given a causal DAG, the causal information is the high-order statistical information which under proper assumptions has asymmetric properties implying direct causes and effects in the data generation process. We categorize such causal information into three levels in order of increasing information content. The lower levels are easier to obtain access to, but they provide less causal information than the higher levels. The different levels of causal information are captured by different forms of causal graphs as illustrated in Fig. 2.

Level 1: Causal skeleton. *Causal skeletons* are the undirected graphs of causal DAGs [Spirtes et al., 2000], and describe the connectivity of nodes. At this level, the causal information in a causal skeleton represents *d-separation* relationships as a type of high-order information. Given a causal DAG, two nodes X and Y are d-separated by a set Z if and only if for each path between X and Y , there is a chain $\cdot \rightarrow Z \rightarrow \cdot$ or a fork $\cdot \leftarrow Z \rightarrow \cdot$ such that Z is in Z ; or it contains a collider $\cdot \rightarrow W \leftarrow \cdot$ such that W and its descendants are not in Z [Peters et al., 2017]. Therefore, given a causal skeleton, we know the nodes that are d-separated; and further under the *causal sufficiency assumption*, i.e., there are no unmeasured confounders (the same common parent of children nodes), the connectivity of two nodes in causal skeletons infers whether a pair of variables are causally dependent or not.

Level 2: Markov equivalent class. At this level, we not only know the d-separation relationships of node pairs, but also know by which node set they are d-separated. Two DAGs are (Markov) equivalent if and only if they have the same d-separation relationships. The Markov equivalent class can be uniquely represented by a completed partially directed acyclic graph (CPDAG) under proper assumptions [Meek, 1995, Andersson et al., 1997], which can provide the full d-separation information alongside certain causal directions, enriching the information of causal skeleton.

Level 3: Causal directed acyclic graph. At this level, all information about the connectivity and causal directions are summarized in causal DAGs. Such causal information is more than knowing all the d-separation relationships. Given the nodes in a causal DAG, we know all of their asymmetric causal relationships, i.e., their direct causes and direct effects.

4 High-Order Structural Causal Benchmark Framework

Reliable and systematic evaluation becomes more and more important for developing and improving current deep generative models, such as the foundation models that can produce confidently incorrect results [Ji et al., 2023]. As an application of deep generative models, tabular data synthesis is also in great need of rigorous evaluation, particularly the intrinsic evaluation that directly measures the quality of synthetic data generated from tabular synthesis models [van Breugel and van der Schaar, 2023]. Metrics based on high-order structural causal information in Sec. 3 can significantly contribute to the intrinsic evaluation. They directly measures the capabilities of tabular synthesis models for capturing causal information that has shown to be important for many machine learning applications [Schölkopf et al., 2021].

However, defining such metrics requires obtaining ground-truth causal labels and identifying causal information, which are in general nontrivial for causal machine learning [Schölkopf et al., 2021]. Therefore, as shown in Fig. 1a, our proposed benchmark framework first generates synthetic benchmark datasets with different data generation processes according to causal graphs that are used for deriving ground-truth causal labels in Sec. 4.1. It then leverages causal discovery methods to identify different levels of causal information¹ and defines high-order metrics at different levels in Sec. 4.2. Additionally, we also use causal inference tasks as downstream tasks for evaluating synthesis models.

¹The first two levels of causal information, causal skeletons and Markov equivalent classes, can be identified by constraint-based causal discovery methods [Spirtes et al., 2000]. The third level of causal information, causal directions, can be further identified by functional causal model-based causal discovery methods [Glymour and Zhang, 2019]. Appendix A provides a brief introduction to causal discovery methods and the identifiability assumptions.

For the sake of clarity, in the following sections, *benchmark datasets* refer to the synthetic benchmark datasets generated according to causal graphs and used for training tabular synthesis models while *synthetic datasets* refer to the datasets generated by the tabular synthesis models.

4.1 Generation of benchmark datasets

The conditions for the validity of benchmark datasets are

- (i) Data are generated according to causal directed acyclic graphs;
- (ii) Based on the data, causal information (causal skeletons or causal directions) is identifiable by causal discovery methods under proper assumptions.

Condition (i) requires that each benchmark dataset has a corresponding causal DAG and a causal DAG can be used for generating a dataset for evaluation. Regarding Condition (i), the data generation process according to a causal DAG is

$$X_i = f_i(X_i^{\text{prt}}, E_{X_i}), \quad (1)$$

where X_i is a variable in the tabular dataset and a node in a causal DAG, X_i^{prt} is the parents of X_i in the graph, f_i is the causal functional relationship between parent and child variables, and E_{X_i} is noise that is independent of X_i^{prt} . Condition (ii) requires that for a benchmark dataset, applying causal discovery methods to it is valid for determining its causal information. Regarding Condition (ii), we limit data generation processes, i.e., the functional relationships and noise distributions in Eqn. (1), to the identifiable ones for causal discovery methods under proper assumptions [Glymour and Zhang, 2019]. Therefore, we categorize the data generation processes by their functional relationships and noise distributions. More specifically, the causal mechanisms of our data generation processes consist of Linear- (L), Sigmoid- (S), and Neural network-based (N) functional relationships (f_i); and Gaussian (G) and Uniform (U) distributions for E_{X_i} . For example, we denote the benchmark dataset generated with a linear functional relationship and Gaussian variables by “LG”. We modify CausalDiscoveryToolbox for randomly generating benchmark datasets with continuous values according to a given causal DAG².

4.2 Benchmark metrics

Benchmark datasets are used for training tabular synthesis models, and their corresponding causal DAGs are used for deriving ground-truth labels of causal information for evaluation. We now define high-order structural causal metrics by applying different causal discovery methods to determine the causal information (which is not available) at different levels from data. Roughly speaking, our metrics compare the references (the differences between ground-truth labels and identified causal information on benchmark datasets) with the differences between ground-truth labels and identified causal information on synthetic datasets; cf. Fig. 1a. Besides causal information on different levels, metrics also indicate model capabilities of capturing joint or individual information, depending on the task. For example, individual causal information can be d-separations and causal directions. Joint causal information is based on the aggregation and integration of individual causal information.

Metrics on causal skeletons. Causal skeletons can be determined by constraint-based causal discovery methods. In our experiments, we apply PC algorithm [Spirtes et al., 2000] to benchmark datasets and synthetic datasets and then get the adjacency matrices of causal skeletons. Furthermore, given the resulting adjacency matrices and the adjacency matrices derived from ground-truth causal DAGs, Structural Hamming Distance (SHD), recall, precision, and F1 score can be used to measure the differences between the resulted and the ground-truth adjacency matrices. Such metrics also indicate model capability of capturing joint causal information, because causal skeletons are constructed by summarizing multiple d-separations.

Metrics on conditional independence relationships. Under causal sufficiency, faithfulness, and causal Markov assumptions, conditional independence in data implies d-separation in a causal graph [Spirtes et al., 2000]. We use conditional independence relationships for benchmarking on the Markov equivalent level. The task based on individual causal information without requiring integrating d-separations. We first select a d-separation and d-connection set with the same set sizes denoted

²Details of the data generation processes are in Appendix C.

by $\mathbf{D} = \{(X_i, Y_i, \mathbf{S}_i)\}_{i=1:N}$, where X_i and Y_i are either d-connected or d-separated conditioning on the set \mathbf{S}_i . We then apply conditional independence tests to the selected subsets of benchmark and synthetic datasets and get results $\mathbf{C}^{\text{ref}} = \{c_i^{\text{ref}} : 0 \text{ or } 1\}_{i \in \mathbf{D}}$ and $\mathbf{C}^{\text{syn}} = \{c_i^{\text{syn}} : 0 \text{ or } 1\}_{i \in \mathbf{D}}$, where 0 and 1 represent conditional dependence and independence respectively; and derive the ground-truth conditional independence relationships from ground-truth causal DAGs denoted by $\mathbf{C}^{\text{gt}} = \{c_i^{\text{gt}} : 0 \text{ or } 1\}_{i \in \mathbf{D}}$. Considering the evaluation on this level as the evaluation of a binary classification problem, Area Under the Curve (AUC) scores of Receiver Operating Characteristic (ROC) curves are used as a metric to measure the difference between $\mathbf{C}^{\text{ref}} / \mathbf{C}^{\text{syn}}$ and \mathbf{C}^{gt} .

Metrics on causal directions. As for methods identifying causal directions, bivariate causal discovery methods [Hoyer et al., 2008, Janzing et al., 2012] are commonly available in software packages. Thus, different from the other metrics, the metric using bivariate causal discovery methods is based on the bivariate setting. We first select a set of edges from the ground-truth causal DAGs denoted by $\mathbf{E} = \{(X_i, Y_i)\}_{i=1:N}$, of which X_i and Y_i are d-separated after removing the edges between them. In this way, we can apply bivariate causal discovery methods to the data of X_i and Y_i without the impact of the other paths between them on the causal direction of the edge between them. We apply bivariate causal discovery methods on the selected subsets of benchmark and synthetic datasets and get the results denoted by $\mathbf{E}^{\text{ref}} = \{e_i^{\text{ref}} : 0 \text{ or } 1\}_{i \in \mathbf{E}}$ and $\mathbf{E}^{\text{syn}} = \{e_i^{\text{syn}} : 0 \text{ or } 1\}_{i \in \mathbf{E}}$; and derive the ground-truth conditional independence relationships from ground-truth causal DAGs denoted by $\mathbf{E}^{\text{gt}} = \{e_i^{\text{gt}} : 0 \text{ or } 1\}_{i \in \mathbf{E}}$, where 0 and 1 represent different causal directions. The metric on this level is the accuracy of the predicted results, \mathbf{E}^{ref} and \mathbf{E}^{syn} , compared to the ground-truth labels \mathbf{E}^{gt} . As a result, the evaluation with bivariate causal discovery methods is based on individual causal information. Besides bivariate causal discovery methods, LiNGAM-based methods [Shimizu et al., 2006, 2011] can be used for identifying causal directions in the multivariate linear non-Gaussian case; hence, SHD, precision, recall, and F1 score can be used as metrics on the resulted fully oriented causal graphs as the ones on the causal skeleton level. This evaluation with LiNGAM-based methods is based on joint causal information.

Metrics on downstream tasks. Downstream tasks are commonly used for evaluating tabular synthesis models. This involves training SCM models on synthetic data and then evaluating their performance on the downstream tasks using unseen data [Zhang et al., 2024, Fang et al., 2024]. We use causal inference tasks, i.e., interventional and counterfactual inference, as downstream tasks, because the performance of models on such tasks relies on capturing essential causal information which is proper for our purpose of benchmarking tabular synthesis models. Our evaluation and metrics are inspired by Chen et al. [2023]. Firstly, benchmark and synthetic data are used for training SCMs given corresponding causal graphs. In the interventional inference task, we perform a series of interventions on each variable in the causal graph, one at a time, and utilize the trained SCM to compute the resulting interventional distributions over the remaining variables. Furthermore, we compute the average differences between the expectation of interventional distributions generated by SCM models trained on synthetic data and benchmark data. For the counterfactual inference task, we generate new observations with the ground-truth SCM for each causal graph. We then compute their counterfactual values with trained SCMs by imposing interventions on each variable individually. The metric is based on the average differences of average counterfactual values between SCM models trained on synthetic data and benchmark data. The metrics are introduced in Sec. 5.1 in detail.

5 Experiments

In this section, we introduce evaluation procedures and experiment setting in Sec. 5.1 and use benchmark datasets and ground-truth causal DAGs for evaluating tabular data synthesis models on high-order structural causal tasks as well as downstream causal inference tasks in Sec. 5.2. Additionally, we also benchmark the baseline methods on causal information with real-world datasets in App. D. Moreover, App. D introduces the configuration of benchmark datasets, other experiment details, and results with other metrics, such as α -precision, β -recall, single variable density estimation score, pair-wise correlation score in [Alaa et al., 2022, Zhang et al., 2024], and the metrics mentioned in Sec. 4.

5.1 Experiment setting

Our baseline methods cover LLM-based and DFM-based methods, which are TabSyn [Zhang et al., 2024], TabDDPM [Kotelnikov et al., 2023], CoDi [Lee et al., 2023], STASY [Kim et al., 2023], TVAE [Xu et al., 2019], and CTGAN [Xu et al., 2019]. Firstly, to benchmark baseline methods on high-order structural causal information, N_g causal DAGs $\mathcal{G}^{\text{gt}} = \{G_g^{\text{gt}}\}_{g=1:N_g}$ are randomly generated and each causal DAG is used for generating benchmark datasets $\mathcal{D}_g^{\text{gt}} = \{D_{g,m}^{\text{gt}}\}_{m \in \omega}$ with different causal mechanisms $\omega = \{\text{LG, LU, SG, NG}\}$. We then train baseline methods on benchmark datasets $D_{g,m}^{\text{gt}}$ and generate synthetic datasets $\mathcal{D}_g^{\text{syn}} = \{D_{g,m}^{\text{syn}}\}_{m \in \omega}$ for each G_g^{gt} . Secondly, with the causal DAGs, benchmark datasets, and synthetic datasets, causal information is identified by causal discovery methods. And causal information, such as adjacency matrices, conditional independence relationships, and predicted edge directions, is denoted by $Q_{g,m}^{\text{ref}} := \text{CD}(D_{g,m}^{\text{gt}})$; $Q_{g,m}^{\text{syn}} := \text{CD}(D_{g,m}^{\text{syn}})$, where CD are causal discovery methods, and ground-truth causal information is derived from causal DAGs, denoted by Q_g^{gt} . We include the results on benchmark datasets as a reference for a fair comparison with the results on synthetic data. Finally, we evaluate baseline methods on causal information with metric $M_i \in \mathcal{M} = \{\text{F1, SHD, others in Sec. 4.2}\}$. Metric values are $R_{g,m}^{\text{ref}} = M_i(Q_{g,m}^{\text{ref}}, Q_g^{\text{gt}})$; $R_{g,m}^{\text{syn}} = M_i(Q_{g,m}^{\text{syn}}, Q_g^{\text{gt}})$. For different evaluation purposes, we can aggregate the metric values along different indices and make conclusions. In our experiments, we compute average metric values over all causal DAGs for each causal mechanism,

$$R_m^{\text{ref}} = \text{AVE}_g(R_{g,m}^{\text{ref}}); R_m^{\text{syn}} = \text{AVE}_g(R_{g,m}^{\text{syn}}).$$

Benchmark on the causal skeleton level. For each causal mechanism, we generate 10 benchmark datasets (according to 10 causal DAGs) with 10 continuous variables and around 17000 samples. For computing metric values, we get 5 bootstrapping datasets with sample size 15000 for each benchmark and synthetic dataset, and apply PC algorithm to get causal information quantities, denoted by $Q_{g,m,b}^{\text{ref}}$ and $Q_{g,m,b}^{\text{syn}}$ where the bootstrapping index is $b = \{1, \dots, 5\}$. The metric value on each causal DAG is the average SHD, recall, precision and F1 scores over 5 bootstrapping datasets, $R_{g,m}^{\text{ref}} = \text{AVE}_{b=1:5}(R_{g,m,b}^{\text{ref}})$; $R_{g,m}^{\text{syn}} = \text{AVE}_{b=1:5}(R_{g,m,b}^{\text{syn}})$. The average and standard deviation of metric values reported in Tab. 1 are computed based on 10 benchmark datasets for each causal mechanism.

Benchmark on the Markov equivalent class level. To evaluate causal information on the Markov equivalent class level, we find all d-separations with minimal conditional sets between each pair of nodes in a causal graph and then apply conditional independence tests to the corresponding sets on synthetic datasets. We use the same procedures as the experiments on causal skeleton level to train baseline methods and generate synthetic datasets. Since we find that the experimental results vary very little across different bootstrapping datasets, we do not use bootstrapping on this level and we use 15000 samples for the tests.

Benchmark on the causal direction level. To test the causal direction by only providing the data of a pair of variables, we select edges between nodes which are d-separated after removing the edge between them. Given such set of edges, we apply bivariate causal discovery algorithms to determine causal directions of them. The sample size for the evaluation is 15000. We use both bivariate causal discovery methods determining causal directions and multivariate causal discovery method determining causal DAGs.

Benchmark on downstream tasks. Our evaluation is inspired by the Chen et al. [2023]. As mentioned in Sec. 4.2, same SCM models are trained on benchmark data and synthetic data together given the underlying causal DAGs. In the interventional inference task, for each causal graph, we take 10 interventions on each variable and approximate the estimated interventional distributions with 1000 samples. In the counterfactual inference task, for each causal graph, we impose 10 interventions on each variable and generate 1000 benchmark data as the new observations for computing counterfactual values. Next, we compare the results on interventional and counterfactual tasks subject to the same interventions. Considering the results of the models trained on benchmark data as the ground-truth results, the metric is the average mean absolute errors (AMAE) over all variables,

$$\text{AMAE-syn} = \frac{1}{V} \sum_{v \in \mathcal{V}} \text{MAE-syn}(v); \text{MAE-syn}(v) = \frac{1}{(V-1) \times K \times N} \sum_{i \in \mathcal{V} \setminus v} \sum_{d \in \mathcal{S}_r} \left| \sum_{s=0}^{N-1} x_{s,d,i}^{\text{ref}} - \sum_{s=0}^{N-1} x_{s,d,i}^{\text{syn}} \right|,$$

where $x_{s,d,i}^{\text{ref}}$ is the reference ground-truth result and $x_{s,d,i}^{\text{syn}}$ is the result of the models trained on synthetic data; s denotes different samples; v denotes that the interventions are imposed on variable v chosen from the variable set \mathcal{V} with V variables; d denotes the intervention value that is taken from

Table 1: Benchmark results with linear Gaussian and linear uniform causal mechanisms. The linear uniform case is visualized by a radar chart in Fig. 1b. Low-order metrics in [Zhang et al., 2024]: Error rate (%) of column density estimation and correlation scores; Causal skeleton level (Skel.): mean and standard deviation of F1 scores; Markov equivalent class level (MEC): AUC of ROC curves; Causal direction level (Dir.): the accuracy of predicting causal directions with bivariate causal discovery methods and the mean and standard deviation of F1 scores with multivariate causal discovery method, LiNGAM. The shaded columns indicate that causal discovery algorithms are not supposed to work in the linear Gaussian case; Metric on the interventional downstream tasks: $100 \times$ average mean absolute errors, denoted by “AMAEs” for short. The complete results with other metrics and causal mechanisms are available in App. D.

(a) Linear Gaussian.

	Low-order		Skel. F1 (\uparrow)	MEC AUC (\uparrow)	Dir.		Intv. AMAE(\downarrow)
	Col. ER (\downarrow)	Pair. ER (\downarrow)			ACC(\uparrow)	F1 (\uparrow)	
ref.	0.00 \pm 0.00	0.00 \pm 0.00	0.90 \pm 0.06	0.972	0.500	0.38 \pm 0.06	3.16 \pm 0.2
TabSyn	2.11 \pm 1.08	0.61 \pm 0.21	0.71 \pm 0.12	0.927	0.500	0.26 \pm 0.07	4.73 \pm 1.8
STASY	12.42 \pm 3.27	1.31 \pm 0.81	0.68 \pm 0.17	0.930	0.696	0.21 \pm 0.07	26.66 \pm 7.1
TabDDPM	0.69 \pm 0.12	0.62 \pm 0.54	0.70 \pm 0.12	0.814	0.536	0.24 \pm 0.09	4.13 \pm 1.2
CoDi	4.42 \pm 0.83	0.80 \pm 0.43	0.72 \pm 0.10	0.917	0.589	0.24 \pm 0.08	5.25 \pm 1.6
GReaT	8.41 \pm 0.73	0.76 \pm 0.26	0.75 \pm 0.04	0.921	0.554	0.36 \pm 0.06	9.77 \pm 0.7
CTGAN	4.70 \pm 0.78	3.76 \pm 0.63	0.46 \pm 0.06	0.566	0.554	0.20 \pm 0.06	15.02 \pm 8.9
TVAE	4.51 \pm 1.64	1.93 \pm 0.64	0.58 \pm 0.06	0.703	0.536	0.20 \pm 0.05	9.52 \pm 5.2

(b) Linear Uniform.

	Low-order		Skel. F1 (\uparrow)	MEC AUC (\uparrow)	Dir.		Intv. AMAE(\downarrow)
	Col. ER (\downarrow)	Pair. ER (\downarrow)			ACC(\uparrow)	F1 (\uparrow)	
ref.	0.00 \pm 0.00	0.00 \pm 0.00	0.89 \pm 0.07	0.967	1.000	0.94 \pm 0.04	3.07 \pm 0.2
TabSyn	1.88 \pm 0.87	0.45 \pm 0.28	0.71 \pm 0.08	0.871	0.946	0.41 \pm 0.06	4.21 \pm 1.1
STASY	11.90 \pm 5.72	1.18 \pm 0.59	0.67 \pm 0.10	0.936	0.946	0.45 \pm 0.10	23.86 \pm 11.1
TabDDPM	0.98 \pm 0.63	1.07 \pm 2.27	0.77 \pm 0.07	0.815	1.000	0.51 \pm 0.14	3.48 \pm 0.6
CoDi	8.01 \pm 1.55	1.75 \pm 1.52	0.74 \pm 0.09	0.902	0.911	0.45 \pm 0.10	3.82 \pm 0.6
GReaT	9.56 \pm 0.73	0.56 \pm 0.22	0.70 \pm 0.05	0.860	0.929	0.57 \pm 0.11	11.20 \pm 1.2
CTGAN	4.71 \pm 0.50	3.52 \pm 0.50	0.51 \pm 0.08	0.588	0.821	0.26 \pm 0.07	10.89 \pm 3.2
TVAE	6.33 \pm 1.69	2.52 \pm 1.17	0.55 \pm 0.07	0.669	0.839	0.29 \pm 0.08	12.22 \pm 3.4

a set \mathcal{S}_r with sample size K ; and i denotes the variable of which the interventional distribution or counterfactual value is computed for evaluation. We compute the mean and standard deviation of the average differences with 10 random seeds.

5.2 Benchmark results and discussion

Benchmark results on different tasks provide different aspects of model capabilities about capturing causal information. To compare baseline methods with an overview of such aspects, we summarize and report the representative results in Tab. 1 and qualitatively visualize the results for the linear uniform case in Fig. 1b. Moreover, the detailed experimental results for all causal mechanisms and metrics in different settings are shown in App. D.

In general, the LLM-based and DFM-based methods can capture the causal information much better than classical deep generative models (TVAE and CTGAN). And TabSyn, CoDi, and TabDDPM are overall competitive baseline methods. But there still exists a gap between the reference and the results of baseline methods. As for the low-order metrics, single column density estimation scores do not always align with high-order structural causal metrics. Methods with poor single column density estimation performance can perform well on some high-order structural causal tasks, such as STASY and GReaT. Correlation scores can be an indication about causal information; whereas, only using it can have misleading conclusions that are different from the evaluation with causal metrics. For example, TabSyn has the best correlation scores and is not the best with many other causal metrics. Moreover, different high-order structural causal metrics can provide different perspectives, such as the ability of capturing individual and joint causal information. GReaT is better at capturing the joint causal information than individual causal information. Because it has better performance on causal skeleton level with PC algorithm and on causal direction level with LiNGAM algorithm, that represents the ability of capturing joint causal information. In contrast, the performance on Markov equivalent class level and causal direction level with bivariate causal discovery methods represents the

ability of capturing individual causal information. And STASY is better at capturing individual causal information. Additionally, the evaluation with downstream tasks considers both density estimation and causal information. TabSyn, CoDi, and TabDDPM have the good performance as they are overall competitive baseline methods with good performance on both low-order metrics and high-order structural causal metrics. STASY and GReaT have the worse results limited by density estimation performance, even though they have reasonably good performance on high-order structural causal task.

6 Conclusion

In this work, we propose a novel benchmark framework for the systematic evaluation of tabular synthesis models on high-order structural information, which paves the way for developing high-order causal-aware tabular synthesis models. We first introduce causal graphs as an important form of prior knowledge in tabular domain and characterize causal information into three levels for defining benchmark tasks and metrics. We then address the problems of the lack of ground-truth labels and the identification of causal information by generating synthetic benchmark datasets and then applying causal discovery methods to extract causal information. Our benchmark framework can distinguish the model capabilities of capturing causal information and provide different perspectives for improving synthesis models. Additionally, evaluation with our benchmark framework can indicate the performance of synthesis models in real-world applications and downstream tasks that depend on causal information. While this work aims at establishing the foundation for benchmarking on causal information, there is room for further improvement. Compelling future work includes expanding the benchmark by including more baseline methods and more structural causal models for generating benchmark datasets.

Acknowledgement

The benchmarking results were enabled by resources provided by the National Academic Infrastructure for Supercomputing in Sweden (NAISS), partially funded by the Swedish Research Council through grant agreement no. 2022-06725.

References

- A. Alaa, B. Van Breugel, E. S. Saveliev, and M. van der Schaar. How faithful is your synthetic data? sample-level metrics for evaluating and auditing generative models. *International Conference on Machine Learning*, 2022.
- S. A. Andersson, D. Madigan, and M. D. Perlman. A characterization of markov equivalence classes for acyclic digraphs. *The Annals of Statistics*, 25(2):505–541, 1997.
- P. Blöbaum, D. Janzing, T. Washio, S. Shimizu, and B. Schölkopf. Cause-effect inference by comparing regression errors. *International Conference on Artificial Intelligence and Statistics*, 2018.
- P. Blöbaum, P. Götz, K. Budhathoki, A. A. Mastakouri, and D. Janzing. Dowhy-gcm: An extension of dowhy for causal inference in graphical causal models. *arXiv preprint arXiv:2206.06821*, 2022.
- R. Bock. MAGIC Gamma Telescope. UCI Machine Learning Repository, 2007. DOI: <https://doi.org/10.24432/C52C8B>.
- R. Bommasani, D. A. Hudson, E. Adeli, R. Altman, S. Arora, S. von Arx, M. S. Bernstein, J. Bohg, A. Bosselut, E. Brunskill, et al. On the opportunities and risks of foundation models. *arXiv preprint arXiv:2108.07258*, 2021.
- A. Bommert, X. Sun, B. Bischl, J. Rahnenführer, and M. Lang. Benchmark for filter methods for feature selection in high-dimensional classification data. *Computational Statistics & Data Analysis*, 2020.
- V. Borisov, T. Leemann, K. Seßler, J. Haug, M. Pawelczyk, and G. Kasneci. Deep neural networks and tabular data: A survey. *IEEE Transactions on Neural Networks and Learning Systems*, 2022.

- T. Brown, B. Mann, N. Ryder, M. Subbiah, J. D. Kaplan, P. Dhariwal, A. Neelakantan, P. Shyam, G. Sastry, A. Askell, et al. Language models are few-shot learners. *Advances in Neural Information Processing Systems*, 2020.
- A. Chen, R. I. Shi, X. Gao, R. Baptista, and R. G. Krishnan. Structured neural networks for density estimation and causal inference. *Advances in Neural Information Processing Systems*, 2023.
- S. Chen. Beijing PM2.5. UCI Machine Learning Repository, 2017. DOI: <https://doi.org/10.24432/C5JS49>.
- T. Chen, T. He, M. Benesty, V. Khotilovich, Y. Tang, H. Cho, K. Chen, R. Mitchell, I. Cano, T. Zhou, et al. Xgboost: extreme gradient boosting. *R package version 0.4-2*, 1(4):1–4, 2015.
- V. Cherepanova, R. Levin, G. Somepalli, J. Geiping, C. B. Bruss, A. G. Wilson, T. Goldstein, and M. Goldblum. A performance-driven benchmark for feature selection in tabular deep learning. *Advances in Neural Information Processing Systems Track on Datasets and Benchmarks*, 2023.
- D. M. Chickering. Optimal structure identification with greedy search. *Journal of machine learning research*, 2002.
- E. Choi, S. Biswal, B. Malin, J. Duke, W. F. Stewart, and J. Sun. Generating multi-label discrete patient records using generative adversarial networks. *Machine Learning for Healthcare Conference*, 2017.
- E. Choi, Z. Xu, Y. Li, M. Dusenberry, G. Flores, E. Xue, and A. Dai. Learning the graphical structure of electronic health records with graph convolutional transformer. In *Proceedings of the AAAI conference on artificial intelligence*, 2020.
- X. Fang, W. Xu, F. A. Tan, J. Zhang, Z. Hu, Y. Qi, S. Nickleach, D. Socolinsky, S. Sengamedu, and C. Faloutsos. Large language models on tabular data—a survey. *arXiv preprint arXiv:2402.17944*, 2024.
- J. A. Fonollosa. Conditional distribution variability measures for causality detection. *Cause Effect Pairs in Machine Learning*, pages 339–347, 2019.
- J. Gardner, Z. Popovic, and L. Schmidt. Benchmarking distribution shift in tabular data with tableshift. *Advances in Neural Information Processing Systems Track on Datasets and Benchmarks*, 2023.
- C. Glymour and K. Zhang. Review of causal discovery methods based on graphical models. *Frontiers in genetics*, 10:418407, 2019.
- L. Grinsztajn, E. Oyallon, and G. Varoquaux. Why do tree-based models still outperform deep learning on typical tabular data? *Advances in Neural Information Processing Systems*, 2022.
- M. Gulati and P. Roysdon. Tabmt: Generating tabular data with masked transformers. *Advances in Neural Information Processing Systems*, 2023.
- L. Hansen, N. Seedat, M. van der Schaar, and A. Petrovic. Reimagining synthetic tabular data generation through data-centric ai: A comprehensive benchmark. *Advances in Neural Information Processing Systems Track on Datasets and Benchmarks*, 2023.
- M. Hernandez, G. Epelde, A. Alberdi, R. Cilla, and D. Rankin. Synthetic data generation for tabular health records: A systematic review. *Neurocomputing*, 2022.
- J. Ho, A. Jain, and P. Abbeel. Denoising diffusion probabilistic models. *Advances in Neural Information Processing Systems*, 2020.
- N. Hollmann, S. Müller, K. Eggenberger, and F. Hutter. TabPFN: A transformer that solves small tabular classification problems in a second. *International Conference on Learning Representations*, 2023.
- P. Hoyer, D. Janzing, J. M. Mooij, J. Peters, and B. Schölkopf. Nonlinear causal discovery with additive noise models. *Advances in Neural Information Processing Systems*, 2008.

- B. Huang, K. Zhang, Y. Lin, B. Schölkopf, and C. Glymour. Generalized score functions for causal discovery. In *Proceedings of the 24th ACM SIGKDD international conference on knowledge discovery & data mining*, 2018.
- D. Janzing, J. Mooij, K. Zhang, J. Lemeire, J. Zscheischler, P. Daniušis, B. Steudel, and B. Schölkopf. Information-geometric approach to inferring causal directions. *Artificial Intelligence*, 2012.
- S. Jesus, J. Pombal, D. Alves, A. Cruz, P. Saleiro, R. Ribeiro, J. Gama, and P. Bizarro. Turning the tables: Biased, imbalanced, dynamic tabular datasets for ml evaluation. *Advances in Neural Information Processing Systems Track on Datasets and Benchmarks*, 2022.
- Z. Ji, N. Lee, R. Frieske, T. Yu, D. Su, Y. Xu, E. Ishii, Y. J. Bang, A. Madotto, and P. Fung. Survey of hallucination in natural language generation. *ACM Computing Surveys*, 2023.
- A. Jolicoeur-Martineau, K. Fatras, and T. Kachman. Generating and imputing tabular data via diffusion and flow-based gradient-boosted trees. *International Conference on Artificial Intelligence and Statistics*, 2024.
- J. Jordon, J. Yoon, and M. Van Der Schaar. Pate-gan: Generating synthetic data with differential privacy guarantees. *International conference on learning representations*, 2018.
- J. Kim, C. Lee, and N. Park. Stasy: Score-based tabular data synthesis. *International Conference on Learning Representations*, 2023.
- A. Kotelnikov, D. Baranchuk, I. Rubachev, and A. Babenko. Tabddpm: Modelling tabular data with diffusion models. *International Conference on Machine Learning*, 2023.
- C. Lee, J. Kim, and N. Park. Codi: Co-evolving contrastive diffusion models for mixed-type tabular synthesis. *International Conference on Machine Learning*, 2023.
- C.-T. Li, Y.-C. Tsai, and J. C. Liao. Graph neural networks for tabular data learning. *International Conference on Data Engineering (ICDE)*, 2023.
- Y. Lipman, R. T. Chen, H. Ben-Hamu, M. Nickel, and M. Le. Flow matching for generative modeling. *International Conference on Learning Representations*, 2023.
- T. Liu, Z. Qian, J. Berrevoets, and M. van der Schaar. Goggle: Generative modelling for tabular data by learning relational structure. *International Conference on Learning Representations*, 2023.
- C. Ma, S. Tschitschek, R. Turner, J. M. Hernández-Lobato, and C. Zhang. Vaem: a deep generative model for heterogeneous mixed type data. *Advances in Neural Information Processing Systems*, 2020.
- A. Malinin, N. Band, Y. Gal, M. Gales, A. Ganshin, G. Chesnokov, A. Noskov, A. Ploskonosov, L. Prokhorenkova, I. Provilkov, et al. Shifts: A dataset of real distributional shift across multiple large-scale tasks. *Advances in Neural Information Processing Systems Track on Datasets and Benchmarks*, 2021.
- C. Meek. Causal inference and causal explanation with background knowledge. In *Proceedings of the Eleventh conference on Uncertainty in artificial intelligence*, 1995.
- P. Morales-Alvarez, W. Gong, A. Lamb, S. Woodhead, S. Peyton Jones, N. Pawlowski, M. Allamanis, and C. Zhang. Simultaneous missing value imputation and structure learning with groups. *Advances in Neural Information Processing Systems*, 2022.
- I. Ng, S. Lachapelle, N. R. Ke, S. Lacoste-Julien, and K. Zhang. On the convergence of continuous constrained optimization for structure learning. *International Conference on Artificial Intelligence and Statistics*, 2022.
- A. Passemiers, P. Folco, D. Raimondi, G. Birolo, Y. Moreau, and P. Fariselli. How good neural networks interpretation methods really are? a quantitative benchmark. *arXiv preprint arXiv:2304.02383*, 2023.
- J. Pearl, M. Glymour, and N. P. Jewell. *Causal inference in statistics: A primer*. John Wiley & Sons, 2016.

- J. Peters, D. Janzing, and B. Schölkopf. *Elements of causal inference: foundations and learning algorithms*. The MIT Press, 2017.
- Z. Qian, R. Davis, and M. van der Schaar. Synthcity: a benchmark framework for diverse use cases of tabular synthetic data. *Advances in Neural Information Processing Systems Track on Datasets and Benchmarks*, 2023.
- A. Radford, J. Wu, R. Child, D. Luan, D. Amodei, I. Sutskever, et al. Language models are unsupervised multitask learners. *OpenAI blog*, 2019.
- M. Scetbon, J. Jennings, A. Hilmkil, C. Zhang, and C. Ma. Fip: a fixed-point approach for causal generative modeling. *arXiv preprint arXiv:2404.06969*, 2024.
- B. Schölkopf, F. Locatello, S. Bauer, N. R. Ke, N. Kalchbrenner, A. Goyal, and Y. Bengio. Toward causal representation learning. In *Proceedings of the IEEE*, 2021.
- A. Sharma and E. Kiciman. Dowhy: An end-to-end library for causal inference. *arXiv preprint arXiv:2011.04216*, 2020.
- S. Shimizu, P. O. Hoyer, A. Hyvärinen, A. Kerminen, and M. Jordan. A linear non-gaussian acyclic model for causal discovery. *Journal of Machine Learning Research*, 2006.
- S. Shimizu, T. Inazumi, Y. Sogawa, A. Hyvarinen, Y. Kawahara, T. Washio, P. O. Hoyer, K. Bollen, and P. Hoyer. Directlingam: A direct method for learning a linear non-gaussian structural equation model. *Journal of Machine Learning Research*, 2011.
- Y. Song and S. Ermon. Generative modeling by estimating gradients of the data distribution. *Advances in Neural Information Processing Systems*, 2019.
- P. Spirtes, C. N. Glymour, and R. Scheines. *Causation, prediction, and search*. MIT press, 2000.
- A. Tsanas and M. Little. Parkinsons Telemonitoring. UCI Machine Learning Repository, 2009. DOI: <https://doi.org/10.24432/C5ZS3N>.
- B. van Breugel and M. van der Schaar. Beyond privacy: Navigating the opportunities and challenges of synthetic data. *arXiv preprint arXiv:2304.03722*, 2023.
- B. van Breugel and M. van der Schaar. Why tabular foundation models should be a research priority. *International Conference on Machine Learning*, 2024.
- A. Vaswani, N. Shazeer, N. Parmar, J. Uszkoreit, L. Jones, A. N. Gomez, Ł. Kaiser, and I. Polosukhin. Attention is all you need. *Advances in Neural Information Processing Systems*, 2017.
- Z. Wang and J. Sun. Transtab: Learning transferable tabular transformers across tables. *Advances in Neural Information Processing Systems*, 2022.
- L. Xu, M. Skoularidou, A. Cuesta-Infante, and K. Veeramachaneni. Modeling tabular data using conditional gan. *Advances in Neural Information Processing Systems*, 2019.
- J. Yan, J. Chen, Y. Wu, D. Z. Chen, and J. Wu. T2g-former: organizing tabular features into relation graphs promotes heterogeneous feature interaction. In *Proceedings of the AAAI Conference on Artificial Intelligence*, 2023.
- H. Zhang, J. Zhang, B. Srinivasan, Z. Shen, X. Qin, C. Faloutsos, H. Rangwala, and G. Karypis. Mixed-type tabular data synthesis with score-based diffusion in latent space. *International Conference on Learning Representations*, 2024.
- K. Zhang and A. Hyvärinen. On the identifiability of the post-nonlinear causal model. *Conference on Uncertainty in Artificial Intelligence*, 2009.
- X. Zheng, B. Aragam, P. K. Ravikumar, and E. P. Xing. Dags with no tears: Continuous optimization for structure learning. *Advances in Neural Information Processing Systems*, 2018.
- Y. Zheng, B. Huang, W. Chen, J. Ramsey, M. Gong, R. Cai, S. Shimizu, P. Spirtes, and K. Zhang. Causal-learn: Causal discovery in python. *Journal of Machine Learning Research*, 2024.

- B. Zhu, X. Shi, N. Erickson, M. Li, G. Karypis, and M. Shoaran. Xtab: Cross-table pretraining for tabular transformers. *International Conference on Machine Learning*, 2023a.
- M. Zhu, K. Kobalcyk, A. Petrovic, M. Nikolic, M. van der Schaar, B. Delibasic, and P. Lio. Tabular few-shot generalization across heterogeneous feature spaces. *arXiv preprint arXiv:2311.10051*, 2023b.

Appendix

Contents

A	A Brief Introduction of Causal Discovery	14
B	Limitations and Future Works	15
C	Data Generation Processes of Benchmark Data	15
D	More Experiments	16
D.1	Hardware, datasets, software, and implementation	16
D.2	More details and benchmarking results	16
D.3	Benchmarking on real-world datasets	17

A A Brief Introduction of Causal Discovery

Causal discovery aims at determining causal relationships purely based on observational data by leveraging their statistical properties under proper assumptions [Spirtes et al., 2000, Peters et al., 2017]. The methodology of causal discovery can be characterized into constraint-based, score-based, and Functional Causal Model (FCM)-based methods [Glymour and Zhang, 2019]. *Constraint-based methods*, such as PC and FCI algorithms, apply conditional independence tests to each pair of variables and infer causal skeletons and causal directions based on certain rules [Spirtes et al., 2000]. *Score-based methods* Chickering [2002], Huang et al. [2018] formulate causal discovery as an optimization problem and optimize score functions by searching in the space of DAGs. Many deep learning-based methods [Zheng et al., 2018, Ng et al., 2022] can be considered as score-based ones. Under Markov and causal faithfulness assumptions, constraint-based and score-based methods identify causal graphs up to certain equivalence classes. For example, suppose that there are no unknown confounders, PC algorithm identifies the Markov equivalence classes of causal DAGs as CPDAGs, and the results of score-based method GES [Chickering, 2002] also converge to Markov equivalence classes. To further identify causal relationships in the same equivalence class, *FCM-based methods* impose additional assumptions of functional classes and distributions on the data generation processes. The most flexible and identifiable FCM is proposed by Hoyer et al. [2008]. Common FCM-based methods [Shimizu et al., 2006, Hoyer et al., 2008] are based on the bivariate case determining the cause and the effect between two variables. For example, one can fit two FCMs in different directions and select the one with large likelihood on the observational data. There are also multivariate FCM-based methods, such as LiNGAM [Shimizu et al., 2006] that assumes that the FCM is a linear non-Gaussian model.

Assumptions of causal discovery methods. Throughout the paper, we frequently mention proper assumptions many times without explicitly stating them. This is because assumptions for different causal discovery methods are always different and some of them involve specific and technical details that makes the paper unnecessarily complicated to follow. For the sake of brevity and clarity, we use "under proper assumptions" in general. The involved assumptions on the causal skeleton level:

- The identifiability conditions of PC algorithm [Spirtes et al., 2000, Peters et al., 2017].

The involved assumptions on the causal direction level:

- The identifiability conditions of additive noise models [Hoyer et al., 2008];
- The identifiability conditions of post-nonlinear models [Zhang and Hyvärinen, 2009];
- The identifiability conditions of LiNGAM [Shimizu et al., 2006].

Potential negative societal impacts. Since real-world scenarios are always violating the assumptions in different ways, the benchmarking results need to be carefully interpreted together with the

causal discovery assumptions. Considering the potential violation of the assumptions for specific applications is necessary for a proper usage of the benchmark framework.

Best Practices in using causal discovery methods for benchmarking on high-order causal structural information. Benchmark datasets with linear relationships and simple distributions (e.g., Gaussian and uniform distributions) are good enough for distinguishing models in terms of capturing causal information. Moreover, the conditional independence tests in constraint-based causal discovery methods can be efficiently applied to datasets with linear relationships; whereas, the kernel-based tests for the datasets with nonlinear relationships are only feasible when the sample size is around 1000. As for the application of bivariate causal discovery methods, we find that the methods without requiring training models are more efficient for the purpose of evaluation and can provide a reasonable evaluation results. And in general, their results do not vary a lot, and do not require bootstrapping for an error bar.

B Limitations and Future Works

This work aims at establishing the foundation of benchmarking tabular synthesis models on causal information and future works can consider to further address some limitations. Firstly, we suggest to expand the benchmark framework with more generation processes (e.g., for discrete and mixed data) while satisfying Conditions (i) and (ii) and include more baseline methods. Current benchmark datasets are based on 10 continuous variables with causal mechanisms *LG*, *LU*, *SG*, and *NG*. Although for the purpose of this paper, it is sufficient with our current setting, it may not be suitable for specific applications or other use cases. Additionally, since this work is based on a general consideration of causal relationships without a specific downstream application, we only choose general benchmark tasks and metrics based on causal discovery algorithms. It is worthwhile to design more task-specific benchmark tasks and metrics when there are specific downstream applications of synthetic tabular data. Moreover, the current experiment setting is too ideal compared with real-world scenarios. More factors can be considered so that benchmark datasets are close to real-world cases. For example, we currently assume that all the variables of a causal graph are known; however, it is not always the case in real-world scenario. And future works can consider to include unknown confounders. Last but not least, our evaluation is limited by the assumptions of causal discovery algorithms, because causal information used for evaluation is not the direct outputs of tabular synthesis models but is extracted by causal discovery methods. For example, we use causal DAGs instead of causal graphs because common causal discovery methods rely on the DAG assumption and the purpose of the work is to evaluate synthesis models, for which the validity is more important than the flexibility of structural causal models. And the mixed data type of continuous and discrete data is not included in the benchmark because there is still lack of studies in causal discovery on such data. This also motivates the research studies in causal discovery domain, which have potentials for modelling tabular data and evaluating synthesis models.

C Data Generation Processes of Benchmark Data

The causal mechanisms for linear, sigmoid, and neural network-based functional relationships are

$$X_i = W_i \cdot X_i^{\text{prt}} + E_{X_i}; \quad (2)$$

$$X_i = W_i \cdot \sigma(X_i^{\text{prt}}) + E_{X_i}; \quad (3)$$

$$X_i = W_{1i} \cdot \sigma(W_{2i} \cdot (X_i^{\text{prt}} \oplus E_{X_i})); \quad (4)$$

where \oplus is concatenation, and W_i , W_{1i} , and W_{2i} are weight matrices.

Even though we leave experiments on discrete data for future works, we provide some suggestions for generating discrete data. To generate a discrete value with K categories of X_i^{disc} , we recommend to first generate a continuous value, then compute the probability of each category as Eqn. (5), and sample from the categorical distribution as Eqn. (6),

$$\text{prob}_k := \text{softmax}(\sigma(W_{i,k} \cdot X_i)); \quad (5)$$

$$X_i^{\text{disc}} \sim \mathcal{C}(\text{prob}_1, \dots, \text{prob}_K), \quad (6)$$

where X_i is a continuous-valued variable, $X_i^{\text{disc.}}$ is a discrete-valued variable, σ is the sigmoid function, $W_{i,k}$ is a random weight for each category of $X_i^{\text{disc.}}$, \mathcal{C} denotes a categorical distribution with parameters prob_k for $k = 1, \dots, K$.

D More Experiments

D.1 Hardware, datasets, software, and implementation

Hardware. We used one NVIDIA RTX 2080 Ti for the benchmarking results.

Implementation of the benchmark framework. Our benchmark framework is available in URL <https://github.com/TURuibo/CauTabBench>.

Baseline methods. The implementation of baseline methods is based on the repository <https://github.com/amazon-science/tabsyn> of [Zhang et al., 2024]. As shown in Tab. 2, we evaluate the synthetic datasets with the metrics in [Zhang et al., 2024] as the reproduced results for a sanity check and a reference for other works. We used the provided training configurations of the dataset "Magic" [Bock, 2007] for training baseline methods.

Benchmark dataset generation. We modify `CausalDiscoveryToolbox` for generating benchmark datasets with randomly generated causal DAGs. For demonstration, we used the configuration, i.e., variable types, the number of variables, and the sample size, of a real-world dataset [Bock, 2007], which is also used for our evaluation on real-world datasets. 10 causal DAGs are randomly generated and each has 10 nodes representing continuous variables and 1 node representing a binary variable. The binary variable in [Bock, 2007] is the classification target variable. For each causal DAG, we generate benchmark datasets of which the sample size is 17117. We find that it is lack of implementation for causal discovery methods in the present of mixed data types; hence, we generate the binary variable independent from all other variables. In this way, we train the baseline methods on 11 variables and evaluate on 10 continuous variables by dropping the binary one, that reduces the influence of the binary variable on the evaluation. We used random seeds from 100 to 109 for generating the 10 causal graphs and their corresponding benchmark datasets.

Causal discovery and inference methods for evaluation. `causal-learn`[Zheng et al., 2024] is used for the evaluation on the causal skeleton level and Markov equivalent class level. The conditional independence test is Fisher’s-Z tests for the datasets with linear relationships and is kernel conditional independence tests for the datasets with nonlinear relationships. `CausalDiscoveryToolbox` is used for the causal direction level. And `DoWhy` [Sharma and Kiciman, 2020, Blöbaum et al., 2022] is used for the evaluation on the causal inference downstream tasks with additive noise models.

Real-world datasets used for the evaluation. We used 4 real-world datasets for the evaluation, which are suitable for our evaluation on the high-order structural causal information. Because they are basically based on linear relationships and continuous variables with a causal semantic context. They are named by Beijing [Chen, 2017], Magic [Bock, 2007], House, and Parkinsons [Tsanas and Little, 2009]. This datasets are licensed under a Creative Commons Attribution 4.0 International (CC BY 4.0) license.

D.2 More details and benchmarking results

The results in Tab 2 show that CoDi stands out for its robust β -recall. However, this model tends to lag in α -precision when compared to state-of-the-art results. On the other hand, TabDDPM and Tabsyn achieve the lowest single column density estimation and pair-wise correlations errors. This suggests their ability to handle also the joint probability distributions between columns. Furthermore, STASY shows limitations in terms of single column density estimation task, having the highest error rates across all datasets and causal mechanisms.

As for benchmarking on the causal skeleton and Markov equivalent class level, we use Fisher’s Z-test and the kernel independence test for datasets with linear and nonlinear functional relationships respectively. Because it is not feasible to apply kernel independence tests to datasets with large sample sizes. Our experiments only include the results with small sample sizes, e.g., 1500. Since

Table 2: Benchmark on low-order statistics. Values are mean and standard deviation of metric values (error rate (%) of single column density, error rate (%) of pair-wise correlation score, α -precision, β -recall) over 10 random causal DAGs.

(a) linear Gaussian					(b) linear uniform				
	Col.	Pair.	α -precision	β -recall		Col.	Pair.	α -precision	β -recall
TabSyn	2.11 \pm 1.08	0.61 \pm 0.21	98.41 \pm 1.39	49.34 \pm 9.09	TabSyn	1.88 \pm 0.87	0.45 \pm 0.28	98.40 \pm 1.01	49.81 \pm 0.95
STASY	12.42 \pm 3.27	1.31 \pm 0.81	93.93 \pm 3.92	43.67 \pm 5.49	STASY	11.90 \pm 5.72	1.18 \pm 0.59	93.71 \pm 5.70	47.37 \pm 2.62
TabDDPM	0.69 \pm 0.12	0.62 \pm 0.54	99.34 \pm 0.14	50.00 \pm 0.40	TabDDPM	0.98 \pm 0.63	1.07 \pm 2.27	99.24 \pm 0.35	41.06 \pm 18.73
CoDi	4.42 \pm 0.83	0.80 \pm 0.43	84.60 \pm 3.13	58.50 \pm 2.02	CoDi	8.01 \pm 1.55	1.75 \pm 1.52	66.48 \pm 2.37	59.84 \pm 2.56
GReaT	8.41 \pm 0.73	0.76 \pm 0.26	81.55 \pm 6.78	51.49 \pm 1.18	GReaT	9.56 \pm 0.73	0.56 \pm 0.22	96.22 \pm 0.84	46.17 \pm 1.09
CTGAN	4.70 \pm 0.78	3.76 \pm 0.63	88.29 \pm 4.09	13.23 \pm 9.09	CTGAN	4.71 \pm 0.50	3.52 \pm 0.50	92.35 \pm 2.37	8.06 \pm 8.69
TVAE	4.51 \pm 1.64	1.93 \pm 0.64	87.17 \pm 9.68	30.77 \pm 10.16	TVAE	6.33 \pm 1.69	2.52 \pm 1.17	92.78 \pm 3.83	14.99 \pm 10.87

(c) sigmoid Gaussian					(d) neural network Gaussian				
	Col.	Pair.	α -precision	β -recall		Col.	Pair.	α -precision	β -recall
TabSyn	1.83 \pm 0.84	0.49 \pm 0.20	98.64 \pm 1.05	49.37 \pm 0.64	TabSyn	1.91 \pm 0.62	0.57 \pm 0.23	98.41 \pm 1.19	48.93 \pm 0.75
STASY	12.48 \pm 5.13	1.52 \pm 0.43	92.77 \pm 6.81	44.83 \pm 3.78	STASY	10.25 \pm 2.80	1.74 \pm 0.87	92.57 \pm 6.11	47.55 \pm 2.99
TabDDPM	0.85 \pm 0.14	0.40 \pm 0.30	99.18 \pm 0.40	49.83 \pm 0.69	TabDDPM	0.75 \pm 0.11	0.30 \pm 0.11	99.16 \pm 0.32	50.27 \pm 0.87
CoDi	5.96 \pm 2.53	1.14 \pm 0.29	92.86 \pm 4.46	61.66 \pm 2.28	CoDi	6.72 \pm 2.73	1.16 \pm 0.59	86.91 \pm 6.90	58.71 \pm 3.76
GReaT	8.51 \pm 2.03	1.45 \pm 0.72	86.12 \pm 5.82	50.65 \pm 2.58	GReaT	7.36 \pm 1.35	1.34 \pm 0.44	87.40 \pm 5.86	48.15 \pm 4.07
CTGAN	4.75 \pm 0.51	3.16 \pm 0.35	89.44 \pm 4.16	23.01 \pm 6.96	CTGAN	4.79 \pm 0.59	3.92 \pm 1.86	89.49 \pm 3.95	11.13 \pm 10.92
TVAE	4.86 \pm 0.93	1.46 \pm 0.50	89.70 \pm 5.98	41.38 \pm 6.49	TVAE	5.27 \pm 1.61	1.78 \pm 0.70	90.38 \pm 6.74	22.04 \pm 15.71

such conditional independence tests are more reliable with larger sample sizes, the performance of baseline methods on the nonlinear datasets is less distinguishable and not as informative as the results on the linear datasets as shown in Tab. 3 and Tab. 4. As for the causal direction level, we apply 3 bivariate causal discovery methods [Janzing et al., 2012, Blöbaum et al., 2018, Fonollosa, 2019] and use the best result of them as the final metric value in Tab. 5.

Table 3: Benchmark on causal skeletons. Values are mean and standard deviation of metric values (SHD, F1 score, recall, and precision) over 10 random causal DAGs. Each metric value on a causal graph is the average value over 5 bootstrapping datasets.

(a) linear Gaussian					(b) linear uniform				
	adj	f1	precision	recall		adj	f1	precision	recall
ref.	3.48 \pm 1.69	0.90 \pm 0.06	0.92 \pm 0.07	0.89 \pm 0.11	ref.	4.04 \pm 2.50	0.89 \pm 0.07	0.91 \pm 0.09	0.88 \pm 0.10
TabSyn	12.96 \pm 4.92	0.71 \pm 0.12	0.88 \pm 0.09	0.61 \pm 0.16	TabSyn	13.16 \pm 5.39	0.71 \pm 0.08	0.89 \pm 0.10	0.60 \pm 0.10
STASY	16.44 \pm 9.19	0.68 \pm 0.17	0.94 \pm 0.07	0.56 \pm 0.19	STASY	14.80 \pm 4.02	0.67 \pm 0.10	0.89 \pm 0.11	0.56 \pm 0.12
TabDDPM	14.16 \pm 8.28	0.70 \pm 0.12	0.86 \pm 0.11	0.61 \pm 0.14	TabDDPM	10.52 \pm 5.37	0.77 \pm 0.07	0.91 \pm 0.09	0.67 \pm 0.10
CoDi	12.32 \pm 3.29	0.72 \pm 0.10	0.92 \pm 0.09	0.60 \pm 0.13	CoDi	11.12 \pm 4.22	0.74 \pm 0.09	0.93 \pm 0.09	0.64 \pm 0.11
GReaT	10.96 \pm 3.53	0.75 \pm 0.04	0.93 \pm 0.08	0.64 \pm 0.05	GReaT	13.48 \pm 5.70	0.70 \pm 0.05	0.87 \pm 0.09	0.60 \pm 0.06
CTGAN	35.04 \pm 5.81	0.46 \pm 0.06	0.88 \pm 0.13	0.32 \pm 0.06	CTGAN	29.60 \pm 6.69	0.51 \pm 0.08	0.89 \pm 0.13	0.37 \pm 0.07
TVAE	23.32 \pm 7.00	0.58 \pm 0.06	0.89 \pm 0.08	0.43 \pm 0.07	TVAE	25.28 \pm 6.56	0.55 \pm 0.07	0.89 \pm 0.12	0.41 \pm 0.06

(c) sigmoid Gaussian (sample size: 1500)					(d) neural network Gaussian (sample size: 1500)				
	adj	f1	precision	recall		adj	f1	precision	recall
ref.	2.04 \pm 1.46	0.95 \pm 0.03	0.94 \pm 0.06	0.95 \pm 0.04	ref.	5.28 \pm 3.15	0.85 \pm 0.07	0.81 \pm 0.15	0.93 \pm 0.07
TabSyn	3.00 \pm 1.20	0.92 \pm 0.02	0.96 \pm 0.04	0.89 \pm 0.05	TabSyn	6.12 \pm 3.36	0.84 \pm 0.06	0.89 \pm 0.08	0.82 \pm 0.09
STASY	4.32 \pm 2.12	0.88 \pm 0.07	0.95 \pm 0.06	0.84 \pm 0.11	STASY	6.32 \pm 3.79	0.83 \pm 0.07	0.81 \pm 0.14	0.87 \pm 0.07
TabDDPM	2.88 \pm 1.26	0.92 \pm 0.03	0.95 \pm 0.06	0.91 \pm 0.06	TabDDPM	5.48 \pm 3.21	0.85 \pm 0.07	0.81 \pm 0.14	0.91 \pm 0.05
CoDi	5.16 \pm 2.29	0.87 \pm 0.06	0.96 \pm 0.05	0.80 \pm 0.11	CoDi	6.68 \pm 2.75	0.82 \pm 0.05	0.86 \pm 0.11	0.82 \pm 0.09
GReaT	4.88 \pm 3.21	0.87 \pm 0.07	0.92 \pm 0.10	0.84 \pm 0.06	GReaT	5.92 \pm 2.28	0.84 \pm 0.05	0.86 \pm 0.09	0.84 \pm 0.07
CTGAN	20.40 \pm 3.58	0.61 \pm 0.05	0.94 \pm 0.07	0.46 \pm 0.06	CTGAN	23.28 \pm 5.63	0.58 \pm 0.04	0.92 \pm 0.08	0.43 \pm 0.04
TVAE	11.12 \pm 4.07	0.75 \pm 0.08	0.96 \pm 0.05	0.63 \pm 0.11	TVAE	14.72 \pm 3.83	0.69 \pm 0.08	0.93 \pm 0.08	0.56 \pm 0.09

Table 4: Benchmark on d-separations: Area under the curve scores (AUC) of ROC curves. sz represents for sample size.

		ref	TabSyn	STASY	TabDDPM	CoDi	GReaT	CTGAN	TVAE
AUC	lg (sz 15000)	0.972	0.927	0.930	0.814	0.917	0.921	0.566	0.703
	lu (sz 15000)	0.967	0.871	0.936	0.815	0.902	0.860	0.588	0.669
	sg (sz 5000)	0.982	0.974	0.963	0.982	0.956	0.964	0.559	0.826
	nn (sz 5000)	0.986	0.890	0.972	0.957	0.909	0.943	0.566	0.752

D.3 Benchmarking on real-world datasets

As for evaluating baseline methods on real-world data, there is no ground-truth causal DAG available \mathcal{G}^{gt} ; hence, we consider the results of causal discovery methods on all the training data as pseudo

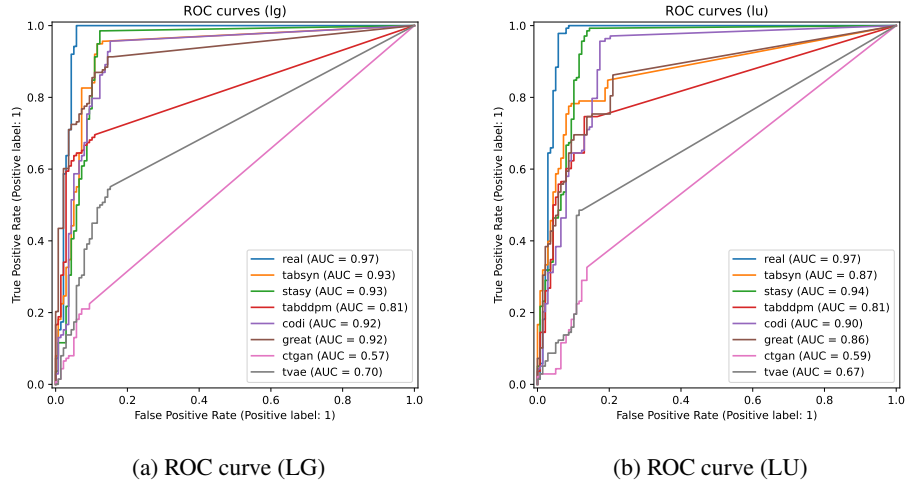


Figure 3: Benchmark on d-separations: ROC curves of the conditional independence test results for Markov equivalent class level evaluation.

Table 5: Benchmark on the causal direction level.

(a) Evaluation with the accuracy (\uparrow) of recovering causal directions. (b) Evaluation with LiNGAM on linear uniform distribution data (bootstrapping times 5).

	LG	LU	SG	NG		SHD (\downarrow)	F1 (\uparrow)
ref.	0.50	1.00	0.96	0.89	ref.	1.04 ± 0.85	0.94 ± 0.04
TabSyn	0.50	0.95	0.98	0.91	TabSyn	21.66 ± 5.75	0.41 ± 0.06
STASY	0.70	0.95	0.96	0.93	STASY	20.66 ± 4.99	0.45 ± 0.10
TabDDPM	0.54	1.00	0.86	0.91	TabDDPM	15.86 ± 8.74	0.51 ± 0.14
CoDi	0.59	0.91	0.89	0.86	CoDi	18.54 ± 5.08	0.45 ± 0.10
GReaT	0.55	0.93	0.91	0.50	GReaT	13.62 ± 9.24	0.57 ± 0.11
CTGAN	0.55	0.82	0.86	0.77	CTGAN	33.64 ± 5.02	0.26 ± 0.07
TVAE	0.54	0.84	0.86	0.80	TVAE	26.62 ± 8.15	0.29 ± 0.08

Table 6: Benchmark on causal directions with LiNGAM on linear uniform with sample size 15000 bootstrapping 5.

	shd	f1	precision	recall
ref.	1.04 ± 0.85	0.94 ± 0.04	0.98 ± 0.03	0.92 ± 0.05
TabSyn	21.66 ± 5.75	0.41 ± 0.06	0.85 ± 0.09	0.28 ± 0.05
STASY	20.66 ± 4.99	0.45 ± 0.10	0.96 ± 0.10	0.30 ± 0.08
TabDDPM	15.86 ± 8.74	0.51 ± 0.14	0.76 ± 0.08	0.39 ± 0.14
CoDi	18.54 ± 5.08	0.45 ± 0.10	0.84 ± 0.15	0.31 ± 0.08
GReaT	13.62 ± 9.24	0.57 ± 0.11	0.84 ± 0.05	0.44 ± 0.11
CTGAN	33.64 ± 5.02	0.26 ± 0.07	0.69 ± 0.22	0.16 ± 0.04
TVAE	26.62 ± 8.15	0.29 ± 0.08	0.63 ± 0.18	0.19 ± 0.05

labels. In this way, conclusions should be made carefully enough, because a worse performance compared with pseudo labels does not necessarily mean that the performance is poor but only represents the relative differences. As shown in Tab. 10, Tabsyn is in general the best model over the four real-world datasets on causal skeleton-level evaluation. Though CoDi and GReaT can perform well on synthetic data, they do not outperform TabSyn in real-world datasets.

We pre-process the real-world dataset, Beijing, and remove the rows with any missing values and the date and time columns with strong correlation (almost deterministic relationship), "year", "month", "day", "hour", and "cbwd".

Table 7: Benchmark on causal directions with LiNGAM on linear Gaussian with sample size 15000 bootstrapping 5.

	shd	f1	precision	recall
ref.	15.42 ± 7.01	0.38 ± 0.06	0.49 ± 0.05	0.32 ± 0.07
TabSyn	27.74 ± 5.14	0.26 ± 0.07	0.51 ± 0.17	0.17 ± 0.05
STASY	31.92 ± 4.55	0.21 ± 0.07	0.45 ± 0.13	0.13 ± 0.06
TabDDPM	26.64 ± 10.34	0.24 ± 0.09	0.42 ± 0.11	0.18 ± 0.08
CoDi	29.66 ± 5.12	0.24 ± 0.08	0.50 ± 0.13	0.16 ± 0.06
GReaT	18.18 ± 8.97	0.36 ± 0.06	0.52 ± 0.08	0.28 ± 0.07
CTGAN	36.00 ± 6.40	0.20 ± 0.06	0.54 ± 0.17	0.13 ± 0.04
TVAE	29.60 ± 8.47	0.20 ± 0.05	0.42 ± 0.12	0.13 ± 0.04

Table 8: Benchmark on interventional and counterfactual tasks with sample size 1000. Values are 100× AMAEs (average mean absolute errors).

(a) Intervention inference.					(b) Counterfactual inference.				
	LG	LU	SG	NG		LG	LU	SG	NG
ref.	3.16 ± 0.2	3.07 ± 0.2	3.3 ± 0.1	3.3 ± 0.2	ref.	0.04 ± 0.0	0.03 ± 0.0	0.32 ± 0.2	0.23 ± 0.1
TabSyn	4.73 ± 1.8	4.21 ± 1.1	4.6 ± 1.1	4.7 ± 0.8	TabSyn	0.56 ± 0.4	0.45 ± 0.7	0.88 ± 0.4	0.90 ± 0.5
STASY	26.66 ± 7.1	23.86 ± 11.1	25.7 ± 10.5	21.3 ± 5.8	STASY	0.65 ± 0.4	0.44 ± 0.3	1.46 ± 0.8	1.63 ± 0.9
TabDDPM	4.13 ± 1.2	3.48 ± 0.6	4.2 ± 0.4	3.8 ± 0.4	TabDDPM	1.12 ± 1.3	0.46 ± 0.7	1.20 ± 0.6	0.75 ± 0.3
CoDi	5.25 ± 1.6	3.82 ± 0.6	10.2 ± 4.2	9.5 ± 3.9	CoDi	0.67 ± 0.8	0.58 ± 0.4	0.94 ± 0.4	1.53 ± 0.7
GReaT	9.77 ± 0.7	11.20 ± 1.2	9.9 ± 3.0	9.3 ± 2.2	GReaT	0.93 ± 0.5	0.58 ± 0.4	1.47 ± 0.6	2.60 ± 1.4
CTGAN	15.02 ± 8.9	10.89 ± 3.2	10.8 ± 2.2	13.0 ± 3.6	CTGAN	8.58 ± 7.7	4.96 ± 3.3	5.02 ± 2.2	7.56 ± 3.8
TVAE	9.52 ± 5.2	12.22 ± 3.4	7.1 ± 1.3	9.4 ± 2.7	TVAE	5.22 ± 3.9	5.40 ± 3.6	2.50 ± 1.4	4.53 ± 2.5

Table 9: Benchmark on low-order statistics on real world datasets. Values are mean and standard deviation of metric values (error rate (%)) of single column density, error rate (%) of pair-wise correlation score, α -precision, β -recall).

(a) Beijing					(b) Magic				
	Col.	Pair.	α -precision	β -recall		Col.	Pair.	α -precision	β -recall
TabSyn	3.69	6.59	99.31	47.96	TabSyn	1.26	0.99	98.17	48.22
STASY	8.22	11.10	93.61	50.12	STASY	6.53	4.28	92.15	49.50
TabDDPM	63.50*	63.29*	0.55*	0.70*	TabDDPM	0.79	1.33	98.66	47.32
CoDi	20.74	6.79	95.35	52.96	CoDi	8.84	5.52	87.20	51.51
GReaT	9.57	60.92	97.36	60.19	GReaT	15.16	9.66	85.17	39.90
CTGAN	19.37	24.89	96.38	39.48	CTGAN	4.43	7.33	90.29	15.13
TVAE	36.53*	40.97*	66.89*	1.69*	TVAE	4.83	6.82	96.22	36.73

(c) House					(d) Parkinsons				
	Col.	Pair.	α -precision	β -recall		Col.	Pair.	α -precision	β -recall
TabSyn	3.76	1.60	95.53	40.41	TabSyn	1.47	22.63	95.08	27.43
STASY	8.27	2.46	96.82	49.31	STASY	28.07	24.84	60.39	21.11
TabDDPMm	1.80	2.11	97.24	47.69	TabDDPMm	1.34	22.79	92.49	27.93
CoDi	26.09	5.69	77.07	34.57	CoDi	11.57	26.61	91.66	38.86
GReaT	18.28	6.17	91.90	37.68	GReaT	7.18	24.36	81.66	29.99
CTGAN	15.71	9.58	51.34	16.08	CTGAN	15.83	17.70	88.57	18.72
TVAE	10.77	4.72	95.37	26.62	TVAE	7.66	6.55	88.86	33.10

Table 10: Benchmark on real world data

(a) Beijing (sample size: 15000)

	SHD	F1	Precision	Recall
ref.	1.20 ± 0.98	0.98 ± 0.02	1.00 ± 0.00	0.96 ± 0.03
TabSyn	9.60 ± 1.74	0.80 ± 0.04	0.74 ± 0.04	0.88 ± 0.06
STASY	2.40 ± 1.20	0.96 ± 0.02	1.00 ± 0.00	0.92 ± 0.04
TabDDPM	19.00 ± 1.00	0.71 ± 0.02	0.88 ± 0.04	0.59 ± 0.01
CoDi	13.40 ± 1.80	0.73 ± 0.03	0.69 ± 0.00	0.77 ± 0.06
GReaT	7.80 ± 1.40	0.84 ± 0.03	0.78 ± 0.04	0.91 ± 0.04
CTGAN	13.80 ± 1.89	0.76 ± 0.03	0.82 ± 0.04	0.70 ± 0.04
TVAE	21.80 ± 2.75	0.53 ± 0.06	0.47 ± 0.05	0.61 ± 0.07

(b) Magic (sample size: 15000)

	SHD	F1	Precision	Recall
ref.	4.40 ± 3.56	0.94 ± 0.05	0.93 ± 0.05	0.95 ± 0.04
TabSyn	9.40 ± 2.20	0.88 ± 0.03	0.86 ± 0.02	0.90 ± 0.04
STASY	12.20 ± 2.89	0.85 ± 0.04	0.83 ± 0.04	0.86 ± 0.05
TabDDPM	17.00 ± 3.38	0.79 ± 0.03	0.82 ± 0.02	0.78 ± 0.05
CoDi	16.40 ± 3.32	0.81 ± 0.04	0.85 ± 0.03	0.77 ± 0.04
GReaT	20.40 ± 2.50	0.75 ± 0.03	0.77 ± 0.02	0.74 ± 0.04
CTGAN	18.80 ± 2.23	0.78 ± 0.02	0.86 ± 0.03	0.73 ± 0.03
TVAE	21.60 ± 3.44	0.73 ± 0.04	0.75 ± 0.06	0.72 ± 0.04

(c) House (sample size: 15000)

	SHD	F1	Precision	Recall
ref.	15.20 ± 3.25	0.90 ± 0.02	0.87 ± 0.03	0.92 ± 0.04
TabSyn	30.80 ± 3.82	0.80 ± 0.02	0.81 ± 0.03	0.79 ± 0.03
STASY	29.00 ± 3.82	0.80 ± 0.03	0.78 ± 0.04	0.83 ± 0.02
TabDDPM	51.40 ± 2.97	0.65 ± 0.02	0.63 ± 0.04	0.67 ± 0.02
CoDi	62.60 ± 3.58	0.61 ± 0.03	0.66 ± 0.04	0.58 ± 0.02
GReaT	64.40 ± 3.67	0.61 ± 0.02	0.66 ± 0.03	0.57 ± 0.02
CTGAN	80.80 ± 1.83	0.58 ± 0.01	0.73 ± 0.02	0.48 ± 0.01
TVAE	43.40 ± 5.73	0.72 ± 0.04	0.75 ± 0.04	0.70 ± 0.04

(d) Parkinsons (sample size: 5000)

	SHD	F1	Precision	Recall
ref.	4.80 ± 3.37	0.91 ± 0.06	0.99 ± 0.03	0.84 ± 0.11
TabSyn	6.60 ± 2.20	0.86 ± 0.04	0.95 ± 0.04	0.80 ± 0.07
STASY	19.60 ± 1.74	0.62 ± 0.02	0.72 ± 0.03	0.54 ± 0.03
TabDDPM	8.20 ± 2.60	0.84 ± 0.04	0.98 ± 0.04	0.74 ± 0.06
CoDi	14.80 ± 2.04	0.72 ± 0.03	0.88 ± 0.04	0.62 ± 0.04
GReaT	13.00 ± 1.84	0.75 ± 0.03	0.88 ± 0.04	0.65 ± 0.04
CTGAN	33.20 ± 3.37	0.46 ± 0.05	0.65 ± 0.07	0.36 ± 0.04
TVAE	22.00 ± 1.26	0.61 ± 0.02	0.79 ± 0.04	0.50 ± 0.02